

PACS numbers: 42.55.Lt; 42.65.Re; 42.65.Jx; 42.65.Ky
DOI: 10.1070/QE2013v043n03ABEH015096

Visible-range hybrid femtosecond systems based on a XeF(C–A) amplifier: state of the art and prospects

S.V. Alekseev, A.I. Aristov, Ya.V. Grudtsyn, N.G. Ivanov, B.M. Koval'chuk, V.F. Losev, S.B. Mamaev, G.A. Mesyats, L.D. Mikheev, Yu.N. Panchenko, A.V. Polivin, S.G. Stepanov, N.A. Ratakhin, V.I. Yalovoi, A.G. Yastremskii

Abstract. **Results of experimental and theoretical investigations of the hybrid (solid state/gas) visible-range femtosecond systems THL-100 (IHCE SB RAS) and THL-30 (P.N. Lebedev Physics Institute) based on a Ti:sapphire front end and a photochemical XeF(C–A) amplifier are reported. The front end generates 50-fs optical pulses with the second-harmonic (475 nm) energy of up to 5 mJ. The active medium of the amplifier is produced in a mixture XeF_2–N_2 subjected to VUV radiation of xenon excited by an electron beam. The computer model is developed for calculating parameters of the XeF(C–A) amplifier, which is in a good agreement with experiments. In the THL-100 system with the 25-cm output aperture of the XeF(C–A) amplifier, a record visible-range femtosecond radiation peak power of 14 GW was obtained in a 50-fs pulse with the time contrast of above 10^8. The measured power of an amplified spontaneous emission of the XeF(C–A) amplifier in the angle of 0.2 mrad was 32 W. The result obtained testifies that the hybrid approach to the development of ultrahigh-power systems provides a high time contrast of radiation (greater than 10^{12} for the projected peak power of 100 TW). In the THL-30 system, prospects for shortening an amplified femtosecond pulse are studied and it is experimentally shown that by compensating a third-order dispersion in a hybrid system one can obtain pulses with duration of at least 27 fs with a recompression of amplified pulses in bulk glass. Also, a new phenomenon was observed of spectrum broadening and self-compression of negatively chirped femtosecond pulses in the visible range under a nonlinear interaction of wide-aperture beams with fused silica. This result opens prospects for development of the new methods of self-compression for femtosecond pulses that are lacking physical limitations on pulse energy and realisation of self-compression of amplified pulses in the output window of the XeF(C–A) amplifier.**

Keywords: *hybrid laser system, XeF(C–A) amplifier, visible-range femtosecond radiation, negatively chirped femtosecond pulse, self-compression.*

S.V. Alekseev, N.G. Ivanov, B.M. Koval'chuk, Yu.N. Panchenko, A.G. Yastremskii Institute of High Current Electronics, Siberian Branch, Russian Academy of Sciences, Akademicheskii prosp. 2/3, 634055 Tomsk, Russia; e-mail: darok@sibmail.com, ivanov.ng@sibmail.com;
V.F. Losev, N.A. Ratakhin Institute of High Current Electronics, Siberian Branch, Russian Academy of Sciences, Akademicheskii prosp. 2/3, 634055 Tomsk, Russia; National Research Tomsk Polytechnic University, prosp. Lenina 30, 634050 Tomsk, Russia; e-mail: losev@ogl.hcei.tsc.ru;
A.I. Aristov, Ya.V. Grudtsyn, S.B. Mamaev, G.A. Mesyats, L.D. Mikheev, S.G. Stepanov, A.V. Polivin, V.I. Yalovoi P.N. Lebedev Physics Institute, Russian Academy of Sciences, Leninsky prosp. 53, 119991 Moscow, Russia; e-mail: mikheev@sci.lebedev.ru

Received 24 January 2013
Kvantovaya Elektronika **43** (3) 190–200 (2013)
Translated by N.A. Raspopov

1. Introduction

Currently, creation of super-high power laser systems with a pulse duration shorter than 100 fs is mainly based on solid-state Ti:sapphire or parametrical amplifiers in the near-IR range and on the technique of amplifying chirped pulses, that is, the pulses stretched in time to the duration of 0.5–1 ns using a linear frequency modulation [1]. After amplification the pulses are compressed back to the initial duration. Pulse stretching is needed for reducing the radiation power below the beam self-focusing threshold value. In solid-state systems the chirp factor is usually $\sim 10^4$. Pulse stretching and compression is performed by diffraction gratings with gold coatings.

In recent years two scientific groups (Institute of High-Current Electronics, SB RAS, Tomsk and P.N. Lebedev Physics institute, RAS, Moscow) actively develop an alternative approach to creation of multi-terawatt and petawatt femtosecond laser systems [2–8]. Those are based on Ti:sapphire femtosecond front ends created at the LPI (second harmonic, λ = 475 nm) [3, 5], the method of optical pumping of gaseous active media on electronic transitions of molecules [9], and nanosecond pulsed energetics and electronics developed at the IHCE SB RAS [10]. To complete the picture one should note that along with the visible-range hybrid systems considered, works on creation of the hybrid systems with the emission wavelength of 248 nm are carried out at the LPI, which are based on e-beam-pumped KrF amplifiers (see, e.g., [11]). An advantage of such a hybrid (solid-state and gaseous media) scheme of powerful femtosecond systems is that, due to a noticeably lower optical nonlinearity of a gaseous active medium as compared to solid-state media the admissible stretch factor for femtosecond pulses prior to amplification is by at least three orders lower than in solid-state systems. Thus, femtosecond pulses stretched into picosecond time domain may be amplified and then compressed by using simpler and more efficient systems, for example, conventional glass (due to a positive group velocity dispersion in the case of a negative chirp) instead of complicated and expensive vacuum grating compressors used in solid-state systems. A gaseous active medium has no physical limitations on scaling and operates in the visible spectral range. The latter circumstance suggests some advantages in the interaction of radiation with plasma and solid targets [8].

Employment of a nonlinear crystal for spectral matching of a solid-state front end with a gaseous medium allows one to realise high-contrast radiation without additional pulse cleaners which is one more important advantage of hybrid systems. Finally, the hybrid system is an alternative to direct nonlinear conversion of IR radiation to the second harmonic for obtaining the pulses with a power of tens or hundreds terawatt in the visible spectral range [12–15].

In the present work we report development of a multiterawatt hybrid laser system THL-100 with an aperture of 24 cm at IHCE SB RAS and present first experimental and theoretical results of investigations of the active medium and amplification conditions for femtosecond radiation. The results of studying key problems of further development of the hybrid concept obtained for the hybrid femtosecond system THL-30 designed at the LPI are also discussed.

2. Hybrid laser system THL-100

2.1. Equipment and measurement methods

Front-end system. As a front end we used a laser system 'Start-480M' produced by Avesta Project Ltd. The system is arranged on an optical table and comprises a Ti : sapphire master oscillator of femtosecond pulses with a 532-nm cw pumpg laser (Verdi-8), stretcher for pulse expansion, regenerative and multipass amplifiers with a 532-nm pulse-periodic pump laser, grating compressor, and second harmonic generator on a KDP crystal. The parameters of the laser beam are as follows: the duration of a transform-limited pulse is 50 fs, the second harmonic pulse (475 nm) energy is up to 5 mJ. The front end operates at a pulse repetition rate of 10 Hz as well as in a single pulse regime with external triggering.

Photodissociation XeF(C–A) amplifier. A photograph of the XeF(C–A) amplifier is given in Fig. 1, and its schematic diagram is presented in Fig. 2. The amplifier comprises two high-voltage pulse generators, a vacuum chamber with an electronic diode, a gas chamber filled with xenon, and the laser cell with a mirror system for multipass amplification of laser pulses.

Figure 1. Photograph of a XeF(C–A) amplifier. The overall dimension is 4.5×1.75×1.75 m.

The pulsed high-voltage generators are linear transformers with a vacuum insulation of a secondary winding; they consist of transforming cascades connected in series [16]. As a primary energy store in each cascade we used four capacitor units connected in parallel. Each unit comprises two capacitors with a total capacity of 80 nF and a six-channel multi-gap spark discharger. The unit capacitors can be charged to 90–100 kV. Secondary windings of the transformers in the vacuum chamber are connected to two cathode holders, each of the latter with

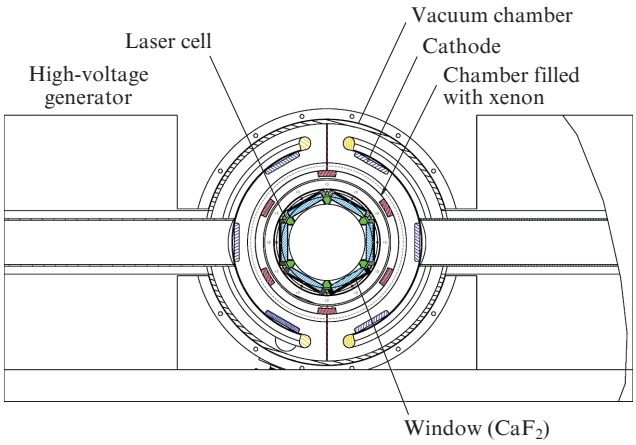

Figure 2. Schematic diagram of the XeF(C–A) amplifier design.

three explosive emission cathodes (flock on metal). All the cathodes are symmetrically arranged around the cylindrical gas chamber 45 cm in diameter. The chamber walls serve as an anode of the vacuum diode and have the form of a mesh made of stainless steel covered by a titanium foil with a thickness of 40 μm. The vacuum diode generates six electron beams (with the cross section of 15×100 cm each), which are injected into the gas chamber filled with xenon at a pressure of 3 atm.

The capacity units charged to 95 kV stored the energy of 34.6 kJ, the electron beam energy in the vacuum diode was ~21 kJ. The energy of the beam passed through the foil to the gas chamber was ~7 kJ. In this case, the accelerator provided the accelerating voltage of 550 kV and diode current of 230 kA at the pulse half-height duration of 150 ns. After injection into the gas chamber the electron beam is almost completely absorbed by xenon in the path length of 8 cm. The electron beam energy is converted into VUV radiation of excimer molecules Xe_2^* with the efficiency of 30%–40% [17].

In the gas chamber there is a hexagon laser cell, in which excimer molecules XeF(B) are produced under the action of a 170-nm VUV radiation due to the photodissociation of XeF_2 molecules. The state (C) of the laser transition XeF(C–A) arises due to relaxation of XeF(B) molecules when the latter collide with molecules of buffer gas N_2. The VUV radiation enters the laser cell through 54 windows arranged on its lateral faces against the mesh with the foil through which the electron beam is injected into the gas chamber. In this way a laser mixture was most efficiently optically pumped with respect to the electron beam energy deposition. The windows of size 12×12 cm are placed in slots on rubber gaskets (viton) and are vacuum-sealed by clamping flanges. From the edges, the cell was closed by the windows made of fused silica with a diameter of 30 cm. The cell cross section was a hexagon with the exit aperture of 24 cm. The laser cell was filled with the gas mixture comprising 0.25–0.5 atm of high-purity nitrogen and 0.1–0.4 Torr of XeF_2 vapours.

For obtaining a maximal efficiency of electron beam energy conversion into VUV radiation, high-purity xenon (99.9997%) was used and the cell was preliminarily evacuated to a pressure of 10^{-4} Torr. Due to electron beam action on constructive elements of the gas chamber, the purity of xenon gradually decreased. The waste xenon was directed to a cleaning system Sircal MP-2000. The number of purifying cycles depends on the number of xenon pump pulses and the duration of its holding time inside the gas chamber.

Experimental methods. The energy of the electron beam and VUV radiation in the laser cell was measured by a TPI-2-7 calorimeter. The small-signal gain was measured in four passes along the active medium of the emission of a cw diode laser SAPPHIRE-488 at the wavelength of 488 nm. The gain distribution over the entire cross section of the laser chamber was measured. The femtosecond laser radiation was amplified by using a multipass optical system (33 passes) comprising 32 circular mirrors with gradually increasing diameters arranged along the perimeter of internal flanges of the laser cell. The beam performed two complete round-trips over the internal perimeter of the laser cell. Prior to entering into the XeF(C–A) amplifier the beam acquired certain divergence by means of a mirror telescope so that the beam diameter increased with amplification from 20 mm (entry) to 62 mm (on the penultimate mirror). The penultimate convex mirror directed the beam onto the plane mirror 100 mm in diameter arranged at the cell axis. After reflection from this mirror the beam passed along the cell axis and escaped the cell. The output beam diameter was 120 mm. The reflection coefficients of the mirrors were 99.5%.

To measure the amplified spontaneous emission (ASE) we focused the output radiation of the XeF(C–A) amplifier with lacking seed femtosecond pulse by a telescopic system with a focal length of 25 m onto a diaphragm 5 mm in diameter, behind which a calibrated photodiode was placed.

In experiments with the 50-fs pulse amplification the latter was expanded in a prism stretcher possessing a negative group velocity dispersion to the duration of ~1650 fs that was calculated by a standard method. An amplified negatively chirped laser pulse was recompressed as the collimated beam of diameter 20 cm twice passed three 4-cm-thick plates made of fused silica, installed at the Brewster angle. The radiation loss in the compressor was at most 2%. A central part of the beam was preliminarily attenuated by reflecting from the faces of two fused silica wedges and then directed by a spherical mirror with a diameter of 90 mm and focal length of 12 m onto an autocorrelator ASF-20-480 for measuring the pulse duration. Prior to entering the autocorrelator, the beam was spatially 'cleaned' by a diaphragm with a diameter of 260 μm placed in a focal waist.

The output energy of the amplifier was measured as follows. The output beam was focused by a positive lens and directed to a wedge made of fused silica, where the beam diameter was 2.5 cm. The energy of the beam reflected from a wedge face was detected by an energy meter OPHIR. An actual energy of the amplified beam was calculated by taking into account a calibrated loss in the detection optical scheme. A photographic paper was placed behind the wedge for detecting a laser beam footprint. The front end was synchronised with the amplifier by a triggering unit with an accuracy of ±10 ns. All the measurements were performed for the first flash of the pump source with a fresh mixture because during the next flash with the same mixture the parameters of the active medium worsened by 20%–30% due to partial decomposition of XeF_2.

Calculation method. The active volume of the amplifier was a cylinder 24 cm in diameter with the length of 110 cm. The gas mixture was $N_2:XeF_2 = 190:0.25$ Torr. The total energy of the pump VUV radiation was 230 J. The pump source was modelled by the cylinder bounding the active medium.

The distributions of particle concentration over r (r is the distance from an observation point to a surface of pump source) at various instants were found by solving the system of integral-differential equations for the transfer of pump VUV radiation and balance equations for the particle concentrations in active medium:

$$\cos\Theta\frac{\partial I(r,t,\Theta)}{\partial r} = -\sigma_{\mathrm{VUV}} I(r,t,\Theta) N, \tag{1}$$

$$\frac{\partial N}{\partial t} = -2\pi N\int_0^{\pi} I(r,t,\Theta)\sin\Theta\,\mathrm{d}\Theta, \tag{2}$$

$$\frac{\partial B(r,t)}{\partial t} = \gamma_{\mathrm{B}} W(r,t) - \tau_{\mathrm{B}}^{-1} B(r,t) + k_{\mathrm{CB}}^{\mathrm{N_2}} C(r,t) M, \tag{3}$$

$$\frac{\partial C(r,t)}{\partial t} = \gamma_{\mathrm{C}} W(r,t) - \tau_{\mathrm{C}}^{-1} C(r,t) + k_{\mathrm{BC}}^{\mathrm{N_2}} B(r,t) M, \tag{4}$$

$$\frac{\partial B_0(r,t)}{\partial t} = \tau_{\mathrm{B}_v}^{-1}(B_0^{\mathrm{e}} - B_0) + k_{\mathrm{B_0C_0}}^{\mathrm{N_2}} C_0(r,x,t) M - \tau_{\mathrm{B}_0}^{-1} B_0(r,t), \tag{5}$$

$$\frac{\partial C_0(r,x,t)}{\partial t} = \tau_{\mathrm{C}_v}^{-1}[C_0^{\mathrm{e}} - C_0(r,x,t)] + k_{\mathrm{C_0B_0}}^{\mathrm{N_2}} B_0(r,t) M - \tau_{\mathrm{C}_0}^{-1} C_0(r,x,t) - \Phi(r,x,t)\sigma C_0(r,x,t), \tag{6}$$

$$\tau_{\mathrm{B}_v}^{-1} = k_{\mathrm{B}_v}^{\mathrm{N_2}} M,\ \tau_{\mathrm{C}_v}^{-1} = k_{\mathrm{C}_v}^{\mathrm{N_2}} M, \tag{7}$$

$$\frac{\mathrm{d}P^{\mathrm{sp}}}{\mathrm{d}x} = h\nu C_0(r,x,t)\frac{\mathrm{d}\Omega}{4\pi} S(x)\tau_{\mathrm{CA}}^{-1}, \tag{8}$$

$$\frac{\partial\Phi(r,x,t)}{\partial x} + \frac{1}{C}\frac{\partial\Phi(r,x,t)}{\partial t} = \Phi(r,x,t)\sigma C_0(r,x,t) + \frac{1}{h\nu}\frac{\mathrm{d}P^{\mathrm{sp}}}{\mathrm{d}x}. \tag{9}$$

Here C_0^{e} and B_0^{e} are the equilibrium concentrations of $XeF(C_0)$ and $XeF(B_0)$ at zero vibration levels; Θ is the angle between the beam propagation direction and normal to the pump source surface; $I(r,t,\Theta)$ is the intensity of VUV pump radiation (photon $\mathrm{cm^{-2}\,s^{-1}}$); σ_{VUV} is the cross section for the pump power absorption by molecules XeF_2; N, B, C, and M are the concentrations of molecules XeF_2, XeF(B), XeF(C), and N_2, respectively; $W(r,t)$ is the number of photolysis acts of XeF_2 per unit volume and unit time; $k_{\mathrm{B}_v}^{\mathrm{N_2}}, k_{\mathrm{C}_v}^{\mathrm{N_2}}$ are the constants of vibration relaxation for the B- and C-states, respectively; γ_{B} and γ_{C} are the quantum yields for producing XeF(B) and XeF(C); $k_{\mathrm{BC}}^{\mathrm{N_2}}, k_{\mathrm{B_0C_0}}^{\mathrm{N_2}}, k_{\mathrm{C_0B_0}}^{\mathrm{N_2}}, k_{\mathrm{CB}}^{\mathrm{N_2}}$ are the collision relaxation rate constants for $XeF(B) + N_2 \rightleftarrows XeF(C) + N_2$ and $XeF(B_0) + N_2 \rightleftarrows XeF(C_0) + N_2$; $\tau_{\mathrm{B}}^{-1} = \tau_{\mathrm{BX}}^{-1} + Q_{\mathrm{B}} + k_{\mathrm{BC}}^{\mathrm{N_2}} M$; $\tau_{\mathrm{C}}^{-1} = \tau_{\mathrm{CA}}^{-1} + Q_{\mathrm{C}} + k_{\mathrm{CB}}^{\mathrm{N_2}} M$; τ_{BX}^{-1} and τ_{CA}^{-1} are the probabilities for spontaneous radiative transitions XeF(B→X) and XeF(C→A);

$$Q_{\mathrm{B}} = \sum_i k_{\mathrm{B}}^{R_i} R_i \text{ and } Q_{\mathrm{C}} = \sum_i k_{\mathrm{C}}^{R_i} R_i$$

are the probabilities of quenching XeF(B) and XeF(C) by mixture components and photolysis products; R_i, $k_{\mathrm{B}}^{R_i}, k_{\mathrm{C}}^{R_i}$ are the corresponding concentrations and rate constants; $\sigma = 9.0\times10^{-18}$ $\mathrm{cm^2}$ [18] is the cross section of stimulated emission on the laser transition; x is the distance from the input window to an observation point along the pulse propagation direction; P^{sp} is the spontaneous emission power in a solid angle $\mathrm{d}\Omega$ at the laser transition frequency; $\Phi(r,x,t)$ is the photon flux at the frequency ν of the laser transition; and c is the speed of light. The seed that forms the photon flux $\Phi(r,x,t)$ is either a spontaneous emission from the layer adjacent to a plane of the input window (when we calculate ASE) or the flux of femtosecond laser radiation injected into the

amplifier (in calculating the laser pulse gain). In each reflection from the mirrors of the multipass amplifier, radiation propagates along an unsaturated medium because the falling and reflected beams propagate in distinct domains. The kinetic equations were solved by using the Gyre approach and the transport equation was solved by the Runge–Kutta method.

Here we present most reliable values for the rate constants of the processes taken into account in the kinetic model: $k_B^{XeF_2} = 5\times10^{-10}$ [19,21], $k_C^{XeF_2} = 2\times10^{-10}$ [19,22], $k_B^{N_2} = 1\times10^{-13}$ [20,22], $k_C^{N_2} = 1\times10^{-13}$ [19,22], $k_{BC}^{N_2} = 4.4\times10^{-11}$ [19,22], ($k_{BC}^{N_2}/k_{CB}^{N_2} = 35$). The radiative lifetimes for the states XeF(C) and XeF(B) are 100 and 14 ns, respectively [20]. The first four constants describe the rate constants of the following processes:

$$\mathrm{XeF(B)} + R_i \xrightarrow{k_B^{R_i}} \text{products},$$

$$\mathrm{XeF(C)} + R_i \xrightarrow{k_C^{R_i}} \text{products}.$$

In the calculation it was assumed that a small-signal gain along the chamber axis is g = const. The optical scheme in the calculation comprised 32 mirrors arranged in such a way that the flux of ASE or the femtosecond laser beam 20 mm in diameter starts near the input window, then it performs 33 passes through the active volume and leaves the latter having a diameter of 62 mm.

In addition, the power of ASE was estimated from the analytical model described in [23]. In this case, the total small-signal gain corresponding to 33 passes through the active medium was the experimental value of 5×10^3.

2.2. Results and discussion

Limiting characteristics of the active medium of the XeF(C–A) amplifier were estimated by measuring the energy of xenon VUV radiation entering the laser cell through the window made of CaF_2. The energy was 230–250 J. Taking into account the energy difference of the pump and amplified radiation quanta, at the 100% quantum efficiency of photodissociation one may assume that the active medium would store the energy of ~90 J. However, according to our calculations due to quenching and spontaneous decay of XeF(C) molecules the stored energy is approximately by an order of magnitude lower and equals ~8 J (Fig. 3).

Preliminary measurements of the active medium gain were performed with a cw laser and the measurement results were compared to the gain of femtosecond pulse radiation. A good correlation of the results was observed. For determining the pump pulse duration we measured the temporal profile of the gain by using the cw laser. The measurements were performed with four passes of probe radiation through the active medium near the windows made of CaF_2 (Fig. 4). One can see that a maximal gain is 0.004 cm^{-1} and the half-height duration of the amplified signal is ~200 ns. Principally, the whole time lapse can be used for amplifying a femtosecond pulse in a multipass optical scheme. Nevertheless, our experiments on femtosecond pulse amplification were only performed in the time range corresponding to a maximal gain. The total duration of amplification for 33 passes was 146 ns.

The measurements of gain show that the latter depends on a concentration of XeF_2 vapours and distance to the laser cell axis. Optimal conditions for femtosecond pulse amplification

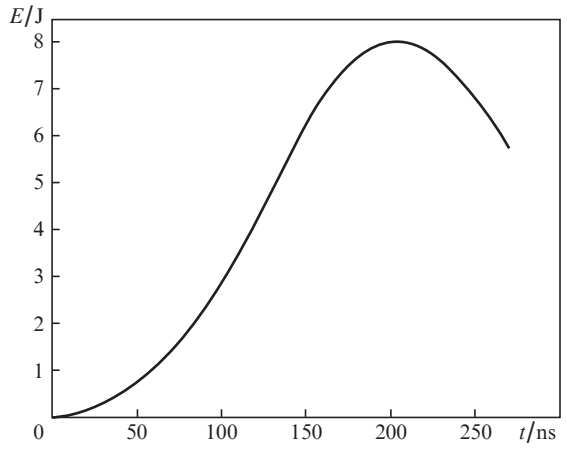

Figure 3. Energy stored in the active medium of amplifier on the upper lasing level of XeF(C) vs. time.

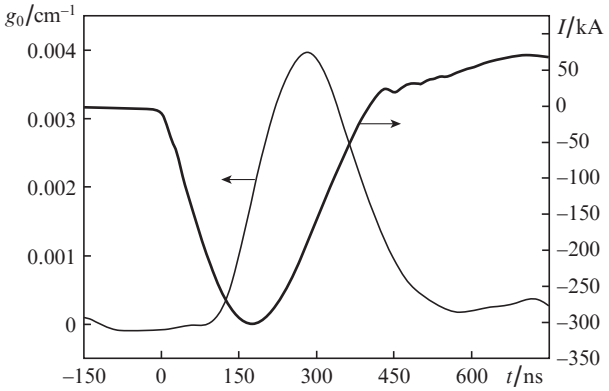

Figure 4. Time profiles of the electron beam current pulse in the diode and gain for cw laser radiation at λ = 488 nm at the pressure of XeF_2 vapour 0.25 Torr near the windows made of CaF_2.

were determined from measurements of a small-signal gain distribution over the cross section of the active medium at various pressures of the XeF_2 vapour (Fig. 5). A calculated gain distribution over radius in the cross section perpendicular to

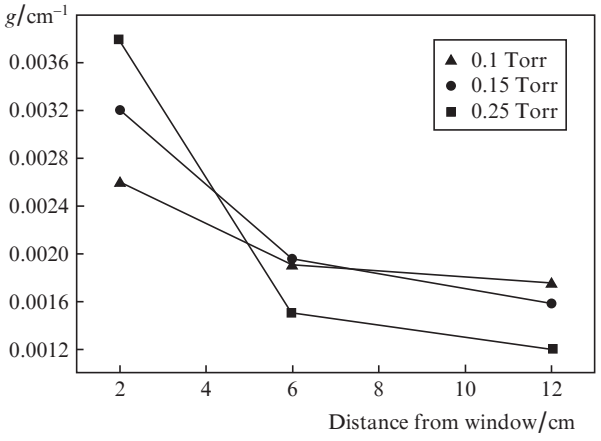

Figure 5. Small-signal gain vs. the distance to a side face of the laser cell (CaF_2 window) at various XeF_2 vapour pressures (experiment). The nitrogen pressure is 190 Torr.

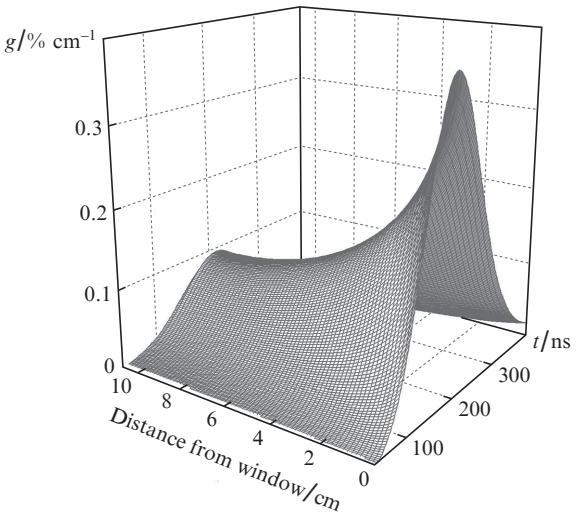

Figure 6. Calculated distribution of the small-signal gain vs. the distance from the side face of the laser cell (CaF_2 window) and time. The pressure of XeF_2 vapour is 0.25 Torr, the nitrogen pressure is 190 Torr.

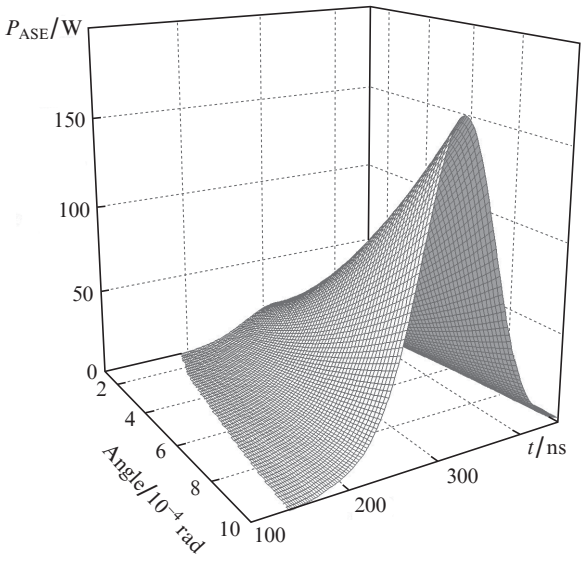

Figure 7. Power of ASE vs. propagation angle and time. The pressure of XeF_2 vapour is 0.25 Torr, the nitrogen pressure is 190 Torr.

the chamber axis is shown in Fig. 6 for various time instants. A good agreement between experimental and calculated data is observed. At a lower vapour pressure the distribution is more uniform; however, the gain in chamber periphery near the CaF_2 windows noticeably falls. The mixture composition was finally optimised by measuring the output energy of amplified femtosecond pulse in a real optical scheme. The resulting maximal energy was obtained at the XeF_2 vapour pressure of 0.2–0.25 Torr.

An important parameter of a femtosecond laser system is a contrast of output radiation. In the present work we measured and calculated the power of ASE, which conventionally limits the value of the contrast. The experiments and calculations were performed for the optimal gas mixture $N_2:XeF_2 = 190:0.25$ Torr. In the calculations we used the experimentally measured spatial gain distribution, the range of ASE propagation angles was from 0.2 to 1 mrad, and the total energy of the pump VUV radiation was 230 J. The calculation results shown in Fig. 7 present the ASE power versus angle and time. One can see that the power in the whole angle is ~175 W. From Fig. 8, one can more accurately determine the ASE power within the angle of 0.2 mrad and compare its time evolution with the pump pulse shape. The power in the angle of 0.2 mrad does not exceed 40 W. The ASE power maximum is observed 150 ns past a maximum of the deposited power. This delay is determined by the radiation propagation time across the multipass resonator.

According to the analytical calculations with employment of experimental data, the ASE power was 25 W, whereas direct ASE power measurements for the XeF(C–A) amplifier at the lasing wavelength within the angle of 0.2 mrad yield 32 W. Thus, a sufficiently good agreement is observed between the experimental and calculated values of the ASE power and one may assert that the latter is no greater than 40 W for the angle of 0.2 mrad.

As was mentioned, the experiments with short pulse amplification were performed with the injected pulse duration of 1650 fs. In this case, the energy at the amplifier entry varied in the range 0.04–2 mJ. The experiments show that in the unsaturated amplification regime the radiation energy increased by a factor of above 5×10^3. In a regime close to a saturated

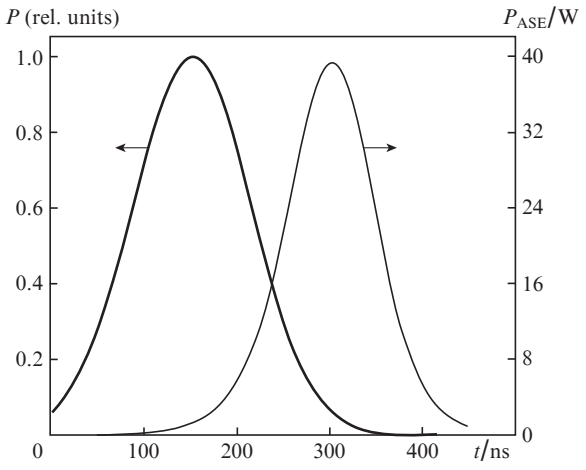

Figure 8. Time evolution of specific pump power P and amplified spontaneous emission power P_{ASE} corresponding to the angle of 0.2 mrad. The pressure of XeF_2 vapour is 0.25 Torr, the nitrogen pressure is 190 Torr.

amplification (50 mJ cm^{-2}), the energy of output radiation increased by a factor of 400–500. Note that the laser beam with the energy of several millijoules injected into the amplifier was not uniform and the uniformity decreased with increasing radiation energy of the front-end system. Beam nonuniformity mainly arising in a nonlinear KDP crystal and the prism stretcher certainly reduces the efficiency of the XeF(C–A) amplifier.

The highest output energy of the amplifier obtained experimentally was 1 J. A footprint of the output laser beam with the pulse energy of 0.7 J is shown in Fig. 9. The pulse duration beyond the compressor was measured at the same energy. First, the pulse was detected that passed the multipass amplifier with lacking pumping, and then a pulse was detected with an excited active medium. In both the cases the detected duration was 50–60 fs (Fig. 10). In view of low loss in the compressor (less than 2%), one may speak about reaching the laser system peak power of 14 TW for a pulse of duration 50 fs.

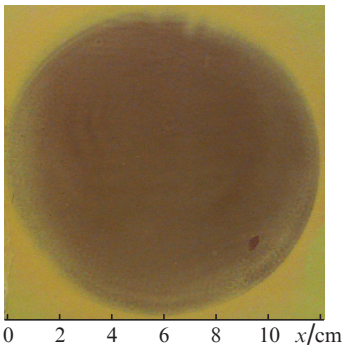

Figure 9. Footprint of the laser beam with the energy of 0.7 J.

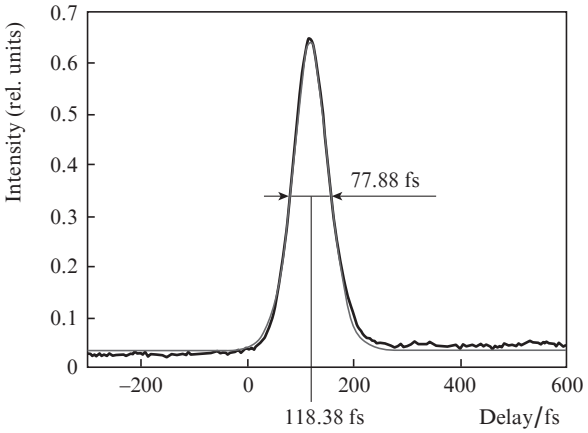

Figure 10. Autocorrelation function of output pulse radiation with the energy of 0.7 J. The pulse duration is 50.5 fs (in the approximation sech^2).

So far as we know the highest output laser radiation power obtained for a XeF(C–A) amplifier is 1 TW [24], and with direct frequency doubling in a Ti:sapphire system a maximal power in the visible spectral range is 4 TW [12]. The ASE power measured (32 W) testifies that the limitation on time contrast for the 14-TW output pulse determined by the XeF(C–A) amplifier is $\sim 4\times 10^{11}$. A real contrast of an amplified pulse is

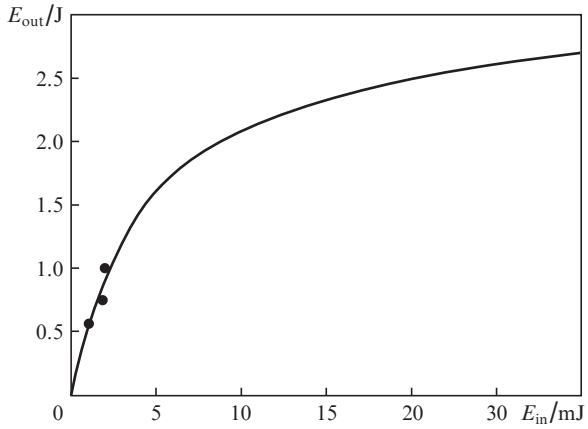

Figure 11. Output energy of XeF(C–A) amplifier vs. energy of input pulse; the curve is a calculation result, points refer to experimental data.

most likely determined by the pulse contrast at an amplifier entry. A typical value of the time contrast in commercial Ti:sapphire systems without special measures for increasing it, is at least 10^4. It means that with the allowance made for a nonlinear frequency doubling the time contrast of radiation at an amplifier entry is above 10^8 and survives in the course of amplification.

In order to predict output parameters of the laser system THL-100 we have calculated the output energy of the XeF(C–A) amplifier versus the input pulse energy. Results of the calculation and of experiments performed are given in Fig. 11. One can see that in increasing the input pulse energy up to 20 mJ the energy at the system output may be 2.5 J.

3. Hybrid laser system THL-30

The system THL-30 created at the LPI (Fig. 12) and thoroughly described in [3] was a prototype for the system THL-100. The seed pulse of femtosecond radiation at the wavelength of 475 nm is also formed in a front-end system 'Start-480M' (Avesta Project Ltd) and has the same parameters as in the system THL-100. The XeF(C–A) amplifier was developed and fabricated at the IHCE SB RAS. It differs from the

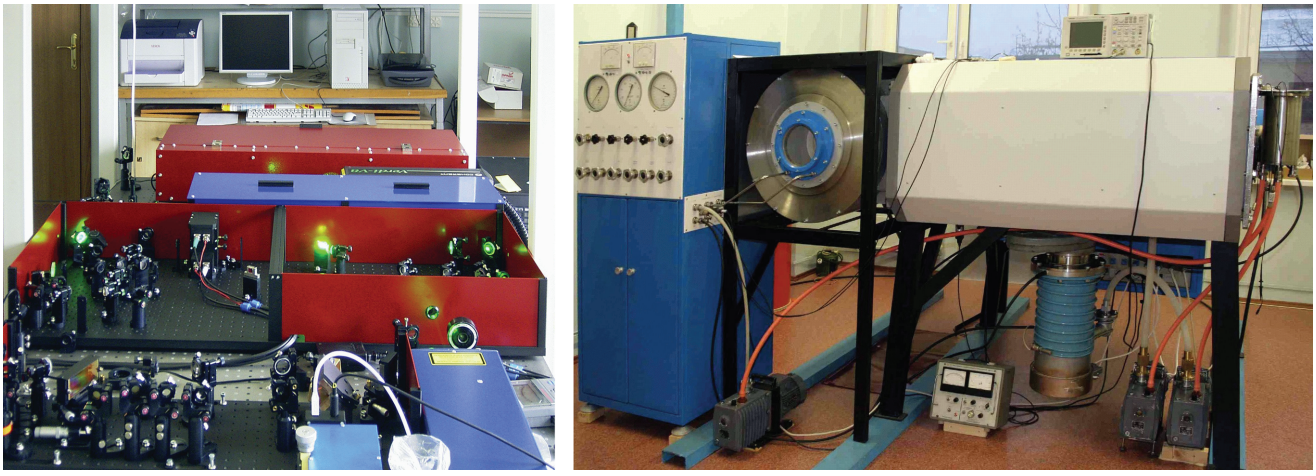

a b

Figure 12. System THL-30: photograph of the front end (a) and XeF(C–A) amplifier (b).

above described one in that the pump source is xenon VUV radiation initiated by four strip electron beams with the cross section of 120×15 cm and total energy behind the foil of 2.5–3 kJ. The corresponding laser chamber has a rectangular cross-section shape with the finishing aperture of 12×12 cm. Results of the experimental investigations of XeF(C–A) amplifier characteristics similar to those for the THL-100 system are presented in [3]. A maximal output energy obtained in the THL-30 system is 0.25 J.

Experiments performed presently with this system are mainly aimed at solving key scientific-technical problems including development of promising technologies and circuitry for further development of the concept of hybrid femtosecond systems. In particular, below are presented results on possible shortening the driving pulse duration in the front-end system and investigations aimed at determining the limiting intensity at which an efficient recompression of negatively chirped pulses in a bulk glass is still possible. It is important for hybrid system scaling and possible performing a recompression of amplified pulses directly in an output window of the amplifier.

3.1. Shortening the driving pulse duration in the front-end system

One of problems arising in development of hybrid systems is compensation of the third-order dispersion in optical elements. The limiting duration of pulses obtained in such systems depends on a solution of the problem. The fact is that in pulse expansion from 50 fs to 1 ps in a two-prism stretcher, the cubic dispersion contribution is negative and is approximately equal to -4×10^4 fs^3 (for glass prisms). Such a value cannot be compensated by a third-order positive dispersion in glass in the course of recompression of amplified pulses. For example, in fused silica the residual cubic dispersion is -2.8×10^4 fs^3, which limits a duration of the pulse that can be restored in the recompression without distortions by the value of ~50 fs. Such duration is actually by an order of magnitude greater than the duration of the pulse that can be amplified in the active medium XeF(C–A) with the gain bandwidth of 70 nm. However, amplification and recompression of shorter pulses require compensation of the third-order dispersion; such compensation can be principally performed by tuning the angle of laser beam incidence onto the compressor gratings in the front end Ti:sapphire system generating femtosecond pulses at a fundamental frequency.

Front end Ti:sapphire systems employed in hybrid femtosecond systems are specific in the output radiation wavelength of 950 nm, which is in a longer wavelength range far from the active medium gain maximum of ~800 nm. Due to a large slope of the spectral curve of the gain cross section near 950 nm, obtaining shorter-duration pulses of a millijoule energy level seems problematic. This is why in the present work we considered the method for broadening a 50-fs pulse at the wavelength of the second harmonic with a following compression to a shorter duration.

A most popular method of spectrum broadening is the self-phase modulation in optical materials possessing a cubic nonlinearity. We have carried out experiments for testing the possibility to compensate a third-order residual dispersion in the scheme comprising two nonlinear elements (a KDP crystal for second harmonic generation and an optical material with a cubic nonlinearity for spectrum broadening). An optical scheme of the experiments is given in Fig. 13.

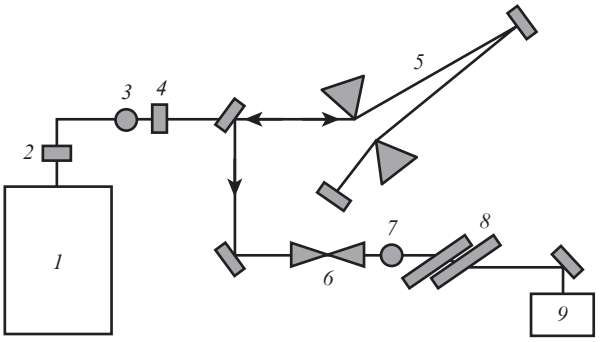

Figure 13. Schematic diagram of the experiment on pulse shortening: (*1*) Ti:sapphire front-end system (λ = 950 nm); (*2*) KDP crystal for second harmonic generation; (*3*) point of optical axis where the spectrum of an initial pulse is measured; (*4*) pile of two plates (fused silica of thickness 8.5 mm and CaF_2 of thickness 13 mm); (*5*) stretcher based on a prism pair; (*6*) spatial filter; (*7*) point of optical axis where the broadened spectrum is measured; (*8*) pile of two glass plates with a total thickness of 13.5 cm; (*9*) autocorrelator.

The grating compressor of the front end Ti:sapphire system was adjusted in such a way that the initial pulse after frequency doubling would have a small positive chirp at the wavelength of 475 nm. The spectrum and autocorrelation function of the initial pulse measured at point (*3*) (Fig. 13) are presented in Fig. 14. The spectral width of the transform-limited pulse approximated by sech^2 corresponds to the dura-

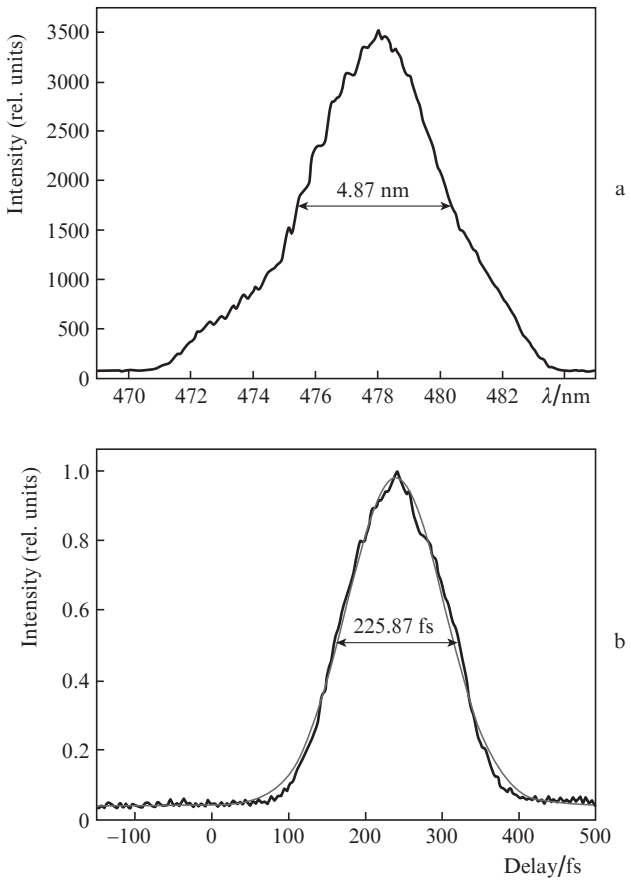

Figure 14. Spectrum (a) and autocorrelation function (b) of an initial pulse. The pulse duration in the Gaussian approximation is 159.7 fs.

tion of 50 fs. The pulse spectrum was broadened by employing two combined plates – a fused silica plate with a thickness of 8.5 mm and a 13-mm thick plate made of CaF_2. The intensity of radiation passing to the plates was 0.1 TW cm^{-2} (the energy was 5 mJ, pulse duration was ~160 fs, and the beam diameter was 8 mm by the level 1/e^2). After spectral broadening the pulse was stretched to 1.3 ps in the prism pair with negative group velocity dispersion and then passed through a spatial filter. The broadened spectrum of the pulse measured after spatial filtering [point (*7*) in Fig. 13] is shown in Fig. 15. Due to a self-phase modulation the spectrum was broadened almost twice, which made it possible to shorten the pulse duration to ~25 fs. Behind the spatial filter the beam diameter increased to 3 cm, which made it possible to perform a reverse time-domain compression in glass in the linear interaction regime (the beam radiation intensity at the end of the compression is ~2 GW cm^{-2}). After the compression in two glass plates with a total thickness of 13.5 cm the pulse was shortened to ~27 fs (Fig. 15). The pulse duration was measured at a central part of a Gaussian beam, which had a diameter of 8 mm.

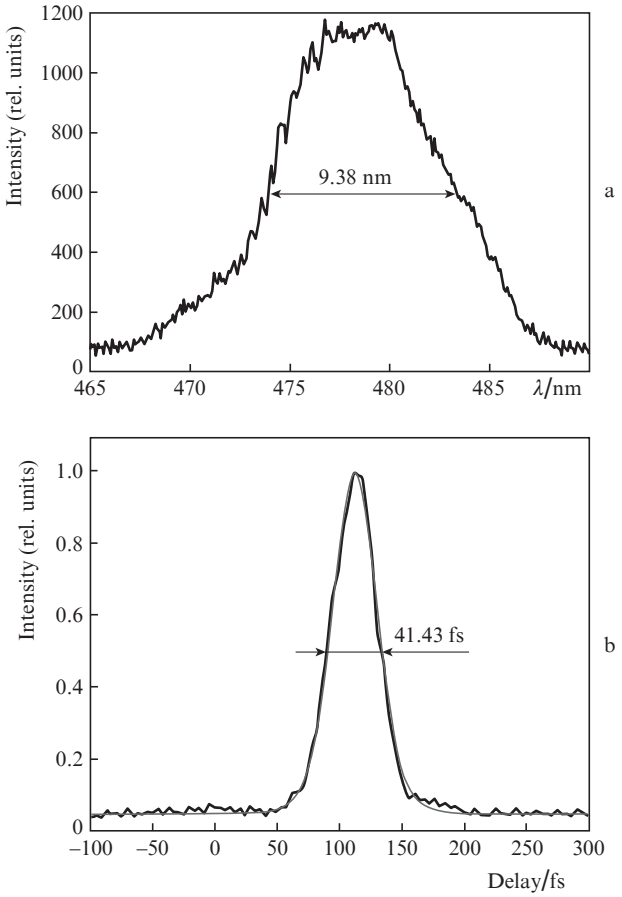

Figure 15. Broadened spectrum of the pulse prior to time-domain compression (a) and autocorrelation function of the pulse after compression in glass (b). The pulse duration in the approximation sech^2 is 26.9 fs.

The result obtained proves that the angle of laser beam incidence on the gratings of the front end Ti:sapphire system corresponded in this experiment to a value of the cubic dispersion, which well enough compensated the residual dispersion after the reverse time-domain compression in a bulk glass. On the other hand, the result testifies that introduction of nonlinear elements into the optical scheme, at least, does not hinder compensation of a residual dispersion in a reverse time-domain compression. Thus, the possibility of pulse duration shortening in hybrid systems to at least 27 fs was experimentally demonstrated.

3.2. Nonlinear compression of femtosecond pulses

Presently, in hybrid systems reverse time-domain compression of negatively chirped pulses in a bulk glass in the visible spectral range is performed in the linear interaction regime to avoid phase distortions while employing Gaussian beams. However, from the viewpoint of the efficiency of energy extraction in the last amplification cascade and an influence of the diffraction at aperture boundaries of transporting optical elements, more promising is employment of super-Gaussian beam profiles with a uniform intensity distribution. In addition, this may increase the beam radiation intensity in the reverse time-domain compression of an amplified pulse in a bulk glass. Hence, it is important to find out the limiting intensities at which negatively chirped pulses can be compressed in bulk transparent optical materials possessing a cubic nonlinearity. For this purpose, the time-domain compression of negatively chirped pulses in bulk fused silica was investigated at intensities of up to 1 TW cm^{-2} and the results were presented in [25].

A schematic diagram of the experiments is shown in Fig. 16. Femtosecond radiation at the wavelength of 475 nm was formed in the Ti:sapphire system 'Start-480M' with frequency doubling (Avesta Project Ltd) that is a part of the hybrid femtosecond visible-range system THL-30. After spatial filtration and passing the double-prism stretcher the beam with the diameter of 1 cm (by the level 1/e) and spectral width of 5.1 nm (Fig. 17) was focused to the sample by a spherical mirror of radius R = 1200 mm. The energy and duration of a negatively chirped pulse behind the stretcher were 0.2 mJ and ~160 fs, respectively. The shape and negative square phase of the femtosecond pulse after the stretcher were controlled by a SPIDER system. The time-domain compression was performed in the plate made of UV fused silica with a thickness of 2.3 mm which was placed behind the focal plane at distances of 2.5, 3, 4, and

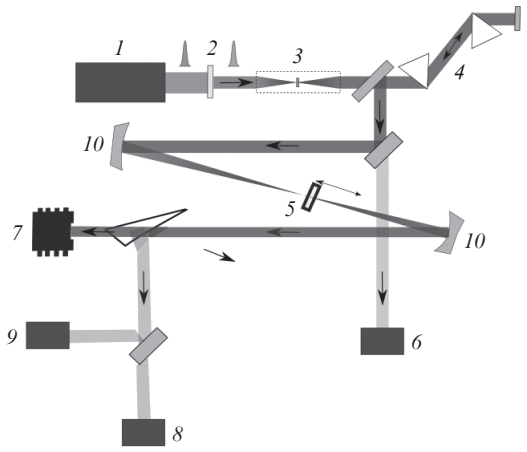

Figure 16. Scheme of the experiment:
(*1*) Ti:sapphire front end 'Start-480M'; (*2*) KDP crystal; (*3*) spatial filter; (*4*) prism stretcher; (*5*) sample; (*6*, *8*) spectrometers; (*7*) calorimeter; (*9*) autocorrelator; (*10*) spherical mirrors of radius 1200 mm.

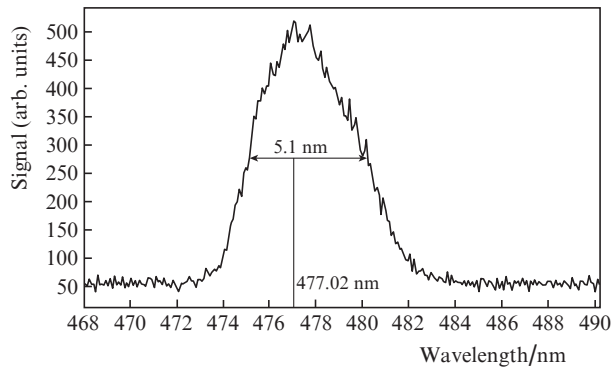

Figure 17. Spectrum of the laser pulse after stretcher prior to focusing.

20 cm from the latter. The beam width by the level 1/e on the sample was 0.42, 0.5, 0.66, and 3.3 mm, respectively, which corresponded to the intensities of 1, 0.6, 0.4 and 0.015 TW cm^{-2} on the sample. In the experiments, the autocorrelation function and spectrum were measured after focusing the radiation in air with the sample and without it. The measurements were performed in the area of maximal radiation intensity, namely, at the beam centre.

The maximal power of laser radiation $P = W/(\sqrt{2\pi}\,\tau_0) =$ 1.2 GW (where τ_0 is the chirped pulse duration) was noticeably lower than the critical self-focusing value in air [26, 27] $P_{cr} = \pi(0.61)^2\lambda^2(1 + C^2)/(8n_0n_2)$, where $C = -2$ is the chirp parameter; $n_2 = 2.4\times10^{-23}$ m^2 W^{-1} is the nonlinear refraction index for air [28]. In addition, interaction with air in this area (the waist diameter is ~20 μm) resulted in an additional nonlinear phase shift of ~1.3 rad, which, however, is unimportant because the effect only necessitates employment of a sample of smaller thickness.

The experimental conditions were chosen so that the wide-aperture approximation was fulfilled at all the intensities, that is, the self-focusing length L_{sf} was substantially greater than the sample thickness. Indeed [26], $L_{sf} = {}^1/_2 d\sqrt{n_0/2n_2I} = 1$ cm, where $d = 0.42$ mm is a minimal beam diameter on a sample at the maximal intensity $I = 1$ TW cm^{-2} and $n_2 = 3.3\times10^{-20}$ m^2 W^{-1} is the nonlinear refraction index of fused silica [29]. However, in view of the fact that the initial pulse is frequency-modulated and the sample placed behind the focal point is illuminated by a diverging beam, the real self-focusing length is well above 1 cm and the wide-aperture approximation is *a fortiori* fulfilled.

Variations of the spectrum and radiation duration in the sample are illustrated in Fig. 18 for various initial intensities. First of all, note that the spectrum shape of an initial pulse actually does not change after passing the focal point. Its width (4.8 nm) corresponds to the duration of a transform-limited 70-fs pulse in the Gaussian approximation. As was already mentioned, the half-height duration of the initial negatively chirped pulse was 160 fs. At $I < 0.7\times10^{12}$ W cm^{-2}, one can see a typical spectral narrowing caused by the self-phase modulation when a negatively-chirped pulse propagates in a medium with a positive group velocity dispersion. Also, the pulse becomes somewhat shorter due to the compensation of the negative quadratic phase of the down-chirped pulse by a positive dispersion of fused silica. At higher intensities the spectrum structure is complicated: Stokes and anti-Stokes components arise and a time-domain self-compression of the pulse to durations of 40–50 fs is observed, which is substantially shorter than the duration of the transform-limited pulse corresponding to the initial spectrum width. In this case, the separation between the intensity peaks in the spectrum reduces: 4.7, 3.8, and 2.7 nm at the intensities of 0.4, 0.7, and 1 TW cm^{-2}, respectively.

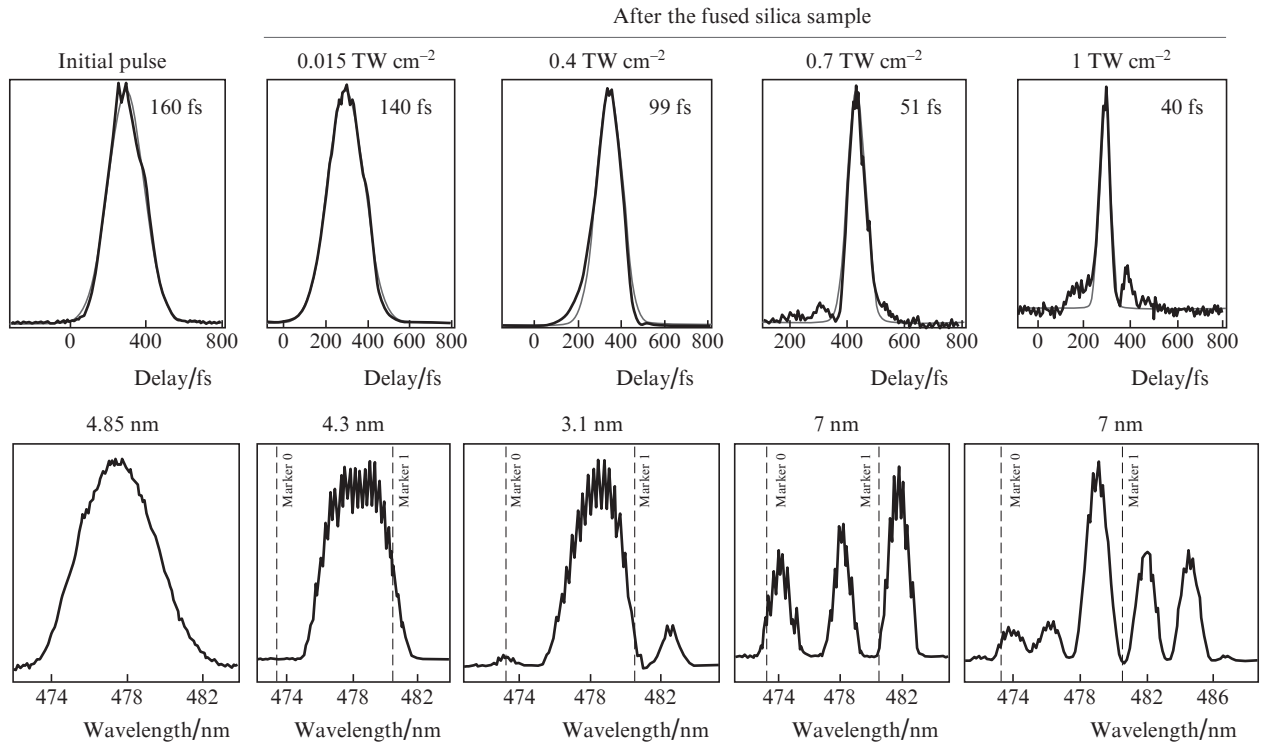

Figure 18. Autocorrelation functions (top) and radiation spectrum (bottom) prior to and after the sample vs. the intensity of incident radiation.

Most probable explanation of the phenomenon is a combined action of the self-phase modulation and four-wave mixing, where the self-modulation affects the time-domain phase of a negatively chirped pulse resulting in formation of a modulated spectrum structure and the four-wave mixing enhances side spectral components. Presently this hypothesis is a basis for more thorough experimental and theoretical investigations.

Thus, for the first time the spectrum broadening was observed in a nonlinear interaction of negatively chirped femtosecond pulses with fused silica, accompanied with a time-domain self-compression of the pulses. One may assume that this phenomenon is specific for many optical materials with a normal dispersion and cubic nonlinearity. The results obtained open prospects for developing a new method of nonlinear time-domain self-compression of wide-aperture beams of femtosecond radiation in optical materials, which is free of the physical limitations on the pulse energy specific for known self-compression methods in filaments and gas-filled capillaries (see, e.g., [30–33]) and has a higher efficiency approaching 100% while using beams with a uniform spatial intensity distribution.

This phenomenon has a particular practical interest for developing recompression methods for femtosecond pulses in the hybrid femto-systems of multi-terawatt-petawatt power in the visible range in which the pulse preliminarily negatively chirped to 1 ps is amplified in gaseous amplifiers under optical pumping. In particular, this may help compression of amplified pulses directly in an output window of a XeF(C–A) amplifier, thus, resigning the employment of compressors at output of hybrid systems.

Note that the nonlinear time-domain self-compression of negatively-chirped femtosecond pulses in optical media with the properties discussed was first observed in [34], where the interaction of the IR radiation at a wavelength of 800 nm with glass of type BK-7 was studied. Though in the experiments of this work the maximal radiation intensity was by a factor of 1.6 higher than in the experiments described above, the authors only observed a weak spectrum narrowing and a change of its shape from Gaussian to Lorentzian, which corresponds to a shorter duration of a transform-limited pulse. The discrepancy between the results is, seemingly, explained by a lower efficiency of the self-action in the IR range.

4. Conclusions

Thus, the hybrid femtosecond laser system THL-100 was built at the IHCE SB RAS, which comprises a Ti:Sapphire front end forming the radiation pulse of duration 50 fs at the wavelength of 475 nm and a XeF(C–A) amplifier with an aperture of 24 cm. The overall small-signal gain in the amplifier was up to 5×10^3. The power of ASE in the amplifier measured in the angle of 0.2 mrad was 32 W. In amplifying the negatively chirped pulse of duration ~1650 fs with the energy of 2 mJ, the output energy of a laser pulse was 1 J. After compressing the output chirped pulse with the energy of 0.7 J, a record high output power of 14 TW with a contrast of above 10^8 was observed for femtosecond radiation at the output of the laser system in the visible range. The computer model was developed capable of calculating active medium parameters for the XeF(C–A) amplifier and ASE. A good agreement was obtained between experiments and calculation results. A numerical simulation shows that the presently projected enhancement of the pulse input energy to 20 mJ may increase the energy of amplified radiation to 2.5 J. In this case, due to the pulse duration shortening to 25 fs the expected peak power should be 100 TW. Taking into account the measured power of ASE and available methods for enhancing the contrast of Ti:sapphire systems there are prospects for obtaining the time contrast of higher than 10^{12}.

The results of the performed investigations on the compensation of third-order dispersion in a hybrid system experimentally prove that the method of amplification of femtosecond pulses negatively chirped in a pair of prisms with a following recompression in a bulk glass allows one to obtain shorter pulses with a duration of at least 27 fs in such systems.

A new phenomenon was discovered, namely, the broadening of spectrum of negatively chirped pulses in the nonlinear interaction with fused silica glass accompanied with a time-domain self-compression of the pulses. This result opens, on the one hand, prospects for developing new self-compression methods for femtosecond pulses which would have no physical limitations on the pulse energy and, on the other hand, the possibility of recompression of amplified pulses in an output window of a XeF(C–A) amplifier, which eliminates the need of final time-domain compressors in hybrid femtosecond systems.

Acknowledgements. The work was supported by the Russian Foundation for Basic Research (Grant Nos 10-02-00121a, 10-08-00022, and 11-08-98050-r_sibir'_a), Federal Target Programme 'Scientists and Science Educators of Innovative Russia' (State Contract No. 02.740.11.0560), programmes of fundamental investigations of the Presidium of RAS 'Problems of Physical Electronics, Charged Particle Beams, and Generation of Electromagnetic Radiation in High-power Systems' and 'Extreme Light Fields and Their Applications' (Project 1.3 and Grant No. 6 of the Siberian Branch of RAS).

References

1. Strickland D., Mourou G.A. *Opt. Commun.*, **56**, 219 (1985).
2. Clady R., Coustillier G., Gastaud M., Sentis M., Spiga P., Tcheremiskine V., Uteza O., Mikheev L.D., Mislavskii V., Chambaret J.P., Chériaux G. *Appl. Phys. B*, **82**, 347 (2006).
3. Aristov A.I., Grudtsyn Ya.V., Zubarev I.G., Ivanov N.G., Krokhin O.N., Losev V.F., Mamaev S.B., Mesyats G.A., Mikheev L.D., Panchenko Yu.N., Rastvortseva A.A., Ratakhin N.A., Sentis M.L., Starodub A.N., Uteza O., Tcheremiskine V.I., Yalovoi V.I. *Opt. Atmos. Okeana*, **22**, 1029 (2009).
4. Losev V., Alekseev S., Ivanov N., Kovalchuk B., Mikheev L., Mesyats G., Panchenko Yu., Ratakhin N., Yastremsky A. *Proc. SPIE Int. Soc. Opt. Eng.*, **7751**, 7751 (09-12) (2010).
5. Alekseev S.V., Ivanov N.G., Koval'chuk B.N., Losev V.F., Mesyats G.A., Mikheev L.D., Panchenko Yu.N., Ratakhin N.A., Yastremskii A.G. *Opt. Atmos. Okeana*, **25**, 221 (2012).
6. Alekseev S.V., Aristov A.I., Ivanov N.G., Koval'chuk B.N., Losev V.F., Mesyats G.A., Mikheev L.D., Panchenko Yu.N., Ratakhin N.A. *Kvantovaya Elektron.*, **42**, 377 (2012) [*Quantum Electron.*, **42**, 377 (2012)].
7. Losev V., Alekseev S., Ivanov N., Koval'chuk B., Mikheev L., Mesyats G., Panchenko Yu., Puchikin A., Ratakhin N., Yastremsky A. *Opt. Prec. Eng.*, **19**, 252 (2011).
8. Mikheev L.D., Tcheremiskine V.I., Uteza O.P., Sentis M.L. *Progr. Quantum Electron.*, **36**, 98 (2012).
9. Mikheev L.D. *Kvantovaya Elektron.*, **32**, 1122 (2002) [*Quantum Electron.*, **32**, 1122 (2002)].
10. Mesyats G.A. *Impul'snaya energetika i elektronika* (Pulsed Energetics and Electronics) (Moscow: Nauka, 2004).
11. Zvorykin V.D., Ionin A.A., Levchenko A.O., Seleznev L.V., Sinitsyn D.V., Ustinovskii N.N. *J. Phys.: Conf. Ser.*, **244**, 032014 (2010).

12. Ozaki T., Kieffer J.-C., Toth R., Fourmaux S., Bandulet H. *Laser Part. Beams*., **24**, 101 (2006).
13. Begishev I.A., Kalashnikov M., Karpov V., Nickles P., Schönnagel H., Kulagin I.A., Usmanov T. *J. Opt. Soc. Am. B*, **21**, 318 (2004).
14. Mironov S., Lozhkarev V., Ginzburg V., Khazanov E. *Appl. Opt*., **48**, 2051 (2009).
15. Ginzburg V.N., Lozhkarev V.V., Mironov S.Yu., Potyomkin A.K., Khazanov E.A. *Kvantovaya Elektron*., **40**, 503 (2010) [*Quantum. Electron*., **40**, 503 (2010)].
16. Koval'chuk B.M., Vizir' V.A., Kim A.A., Kumpyak E.V., Loginov S.V., Bastrikov A.N., Chervyakov V.V., Tsoi N.V., Monzho F., Khyu D. *Izv. Vyssh. Uchebn. Zaved., Ser. Fiz*., **40**, 25 (1997).
17. Eckstrom D.J., Walker H.C., Jr. *IEEE J. Quantum Electron*., **QE-18**, 176 (1982).
18. Bischel W.K., Eckstrom D.J., Walker H.C. Jr., Tilton R.A. *J. Appl. Phys*., **52**, 4429 (1981).
19. Tcheremiskine V.I. *Ph.D Thesis* (Universite de la Mediterranee, Marseille, 1999).
20. Black G., Sharpless R.L., Lorents D.C., Huestis D.L., Gutchek R.A., Bonifield T.D., Helms D.A., Walters G.K. *J. Chem. Phys*., **75**, 4840 (1981).
21. Bibinov N.K., Vinogradov I.P., Mikheev L.D., Stavrovskii D.B. *Kvantovaya Elektron*., **8**, 1945 (1981) [*Sov. J. Quantum Electron*., **11**, 1178 (1981)].
22. Brashears H.C., Setser D.W. *J. Chem. Phys*., **76**, 4932 (1982).
23. Basov N.G., Grasyuk A.Z., Zubarev I.G. *Zh. Prikl. Spektrosk*., **3**, 26 (1965).
24. Hofmann Th., Sharp T.E., Dane C.B., Wisoff P.J., Wilson W.L. Jr., Tittel F.K., Szabo G. *IEEE J. Quantum Electronics*, **28**, 1366 (1992).
25. Aristov A.I., Grudtsyn Ya.V., Mikheev L.D., Polivin A.V., Stepanov S.G., Trofimov V.A., Yalovoi V.I. *Kvantovaya Elektron*., **42**, 1097 (2012) [*Quantum Electron*., **42**, 1097 (2012)].
26. Boyd R.W. *Nonlinear Optics* (San Diego, CA: Academic Press, 1992).
27. Cao X.D., Agrawal G.P., McKinstrie C.J. *Phys. Rev. A*, **49**, 4085 (1994).
28. Loriot V., Hertz E., Faucher O., Lavorel B. *Opt. Express*, **17**, 13429 (2009).
29. Milam D. *Appl. Opt.*, **37**, 546 (1998).
30. Varela O., Alonso B., Sola I.J., San Román J., Zaïr A., Méndez C., Roso L. *Opt. Lett*., **35**, 3649 (2010).
31. Kurilova M.V., Uryupina V.S., Mozhorova A.V., Volkov R.V., Gorgutsa S.R., Panov N.A., Kosareva O.G., Savel'ev A.B. *Kvantovaya Elektron*., **39**, 879 (2009) [*Quantum Electron*., **39**, 879 (2009)].
32. Skobelev S.A., Kulagin D.I., Stepanov A.N., Kim A.V., Sergeev A.M., Andreev N.E. *Pis'ma Zh. Eksp. Teor. Fiz*., **89**, 641 (2009).
33. Skobelev S.A., Kim A.V., Willi O. *Phys. Rev. Lett*., **108**, 123904 (2012).
34. Liu J., Chen X., Liu J., Zhu Y., Leng Y., Dai J., Li R., Xu Z. *Opt. Express*, **14**, 979 (2006).